ANALYSIS USING SURFACE WAVE METHODS TO DETECT SHALLOW MANMADE TUNNELS

Niklas H. Putnam[1] (nhp270@mst.edu; 573-337-8090), Ali Nasseri-Moghaddam[3] (a.nasserim@gmail.com; 519-725-9328), Oleg Kovin[1] (onktg6@mst.edu; 573-341-6047), Evgeniy Torgashov[1] (evtct3@mst.edu; 573-202-8958), Neil L. Anderson[1] (nanders@mst.edu; 573-341-4852), S. Grant[2] (sgrant@mst.edu; 573-341-4893),
[1]Department of Geological Sciences and Engineering; [2]Department of Electrical Engineering, Missouri University of Science & Technology, Rolla, Missouri, 65409
[3]Inspec-Sol Inc., 651 Colby Drive, Waterloo, ON N2V 1V6, Canada

Abstract

Multi-channel Rayleigh wave data were acquired across a 1 m diameter spillway tunnel along three parallel traverses with surface to tunnel separations of 0.90 m, 2.15 m and 3.13 m depth, respectively. These surface wave data were acquired by placing a 24-channel geophone array perpendicular to the center-line of the spillway tunnel and incrementally moving the array across the tunnel. The near source-receiver offset was 6 m; the 4.5 Hz geophones were spaced at 0.5 m. The tunnel locations were identified visually on velocity-filtered common-shot gathered field records. Tunnel locations were also identified by analyzing common shot-gathered records using two newly-developed automated interpretation programs: Spiking Filter Analysis and Attenuation Analysis of Rayleigh Waves (AARW). Electrical resistivity data was acquired along each traverse for comparison purposes.

Introduction

The engineering geophysics community has recently focused on the use of Rayleigh (surface) wave methods, such as Multichannel Analysis of Surface Waves (MASW) and Refraction Micrometer (ReMi), to detect manmade tunnels in the earth's shallow subsurface (Miller et al., 2006). Successful tunnel-detection applications of these methods have been reported. However, further experimental and analytical investigations are required to comprehend all significant aspects of the observed surface wave data. This case study reports on three alternate surface wave methods that were used to locate a 1 m diameter tunnel: visually-identified diffracted/reflected surface–wave energy; the Attenuation Analysis of Rayleigh Wave (AARW); and Spiking Filter Analysis.

The study site is located at Ber Juan Park in the City of Rolla, Missouri about 172 kilometers (107 miles) southwest of St. Louis off of U.S. Interstate Highway 44. According to design specifications, the tunnel is a reinforced concrete lined spillway pipe, 1.07 m in diameter with a 1.5 percent gradient downstream. The reinforced concrete liner is 0.06 m thick with an internal diameter of 0.94 m. The spillway was sealed using a compacted high plastic clay backfill around the pipe to 0.25 m. The earthen dam containing the spillway pipe is composed of compacted local clayey fill with

Report Documentation Page

Form Approved
OMB No. 0704-0188

1. REPORT DATE	2. REPORT TYPE	3. DATES COVERED
01 DEC 2008	**N/A**	**-**

4. TITLE AND SUBTITLE	5a. CONTRACT NUMBER
Analysis Using Surface Wave Methods To Detect Shallow Manmade Tunnels	5b. GRANT NUMBER
	5c. PROGRAM ELEMENT NUMBER
6. AUTHOR(S)	5d. PROJECT NUMBER
	5e. TASK NUMBER
	5f. WORK UNIT NUMBER
7. PERFORMING ORGANIZATION NAME(S) AND ADDRESS(ES) **Department of Geological Sciences and Engineering Missouri University of Science & Technology, Rolla, Missouri, 65409**	8. PERFORMING ORGANIZATION REPORT NUMBER
9. SPONSORING/MONITORING AGENCY NAME(S) AND ADDRESS(ES)	10. SPONSOR/MONITOR'S ACRONYM(S)
	11. SPONSOR/MONITOR'S REPORT NUMBER(S)

12. DISTRIBUTION/AVAILABILITY STATEMENT
Approved for public release, distribution unlimited

13. SUPPLEMENTARY NOTES
See also ADM002187. Proceedings of the Army Science Conference (26th) Held in Orlando, Florida on 1-4 December 2008, The original document contains color images.

14. ABSTRACT

15. SUBJECT TERMS

16. SECURITY CLASSIFICATION OF:			17. LIMITATION OF ABSTRACT	18. NUMBER OF PAGES	19a. NAME OF RESPONSIBLE PERSON
a. REPORT	b. ABSTRACT	c. THIS PAGE			
unclassified	**unclassified**	**unclassified**	**UU**	**10**	

6 to 12 inch stone. The spillway pipe did not contain water at the time of the geophysical survey.

The primary objective of this case study was to determine the utility and reliability of the automated Spiking Filter and AARW methods for shallow tunnel detection. The tunnel locations output by the automated interpretations were compared to the spillway blueprints to assess accuracy. Electrical resistivity profiles were acquired along the surface-wave traverses for comparison purposes.

Figure 1: (a) 4.5 Hz geophone array over spillway tunnel at a Ber Juan Park, Rolla, MO.: Graduate student Wamweya uses a sledge hammer source to generate surface wave energy. (b) Design blueprints and on-site measurements of the Ber Juan spillway pipe are compared to the geophysical interpretations to assess the reliability of automated interpretation methods.

Resistivity

An AGI SuperSting automated resistivity system was used to image the subsurface across the spillway tunnel along the surface wave traverses (Figure 2). A dipole-dipole array was employed. Electrodes were spaced at 0.5 m (for the 0.90 m and 2.15 m depths tests) and at 1 m (for the 3.13 m depth test). The air-filled tunnel is represented as a zone of anomalously high resistivity on the three profiles (Figure 2). The resistivity profiles, as a whole, exhibit relative homogeneity below the thin layer of dry capping soil Resistivities in the range of 15 to 20 Ωm are consistent with clayey compacted fill (Reynolds, 2000; p. 442). The interpretation of the resistivity data supports that the subsurface geology at Ber Juan is effectively uniform (except for the tunnel) and therefore an ideal field laboratory for this study.

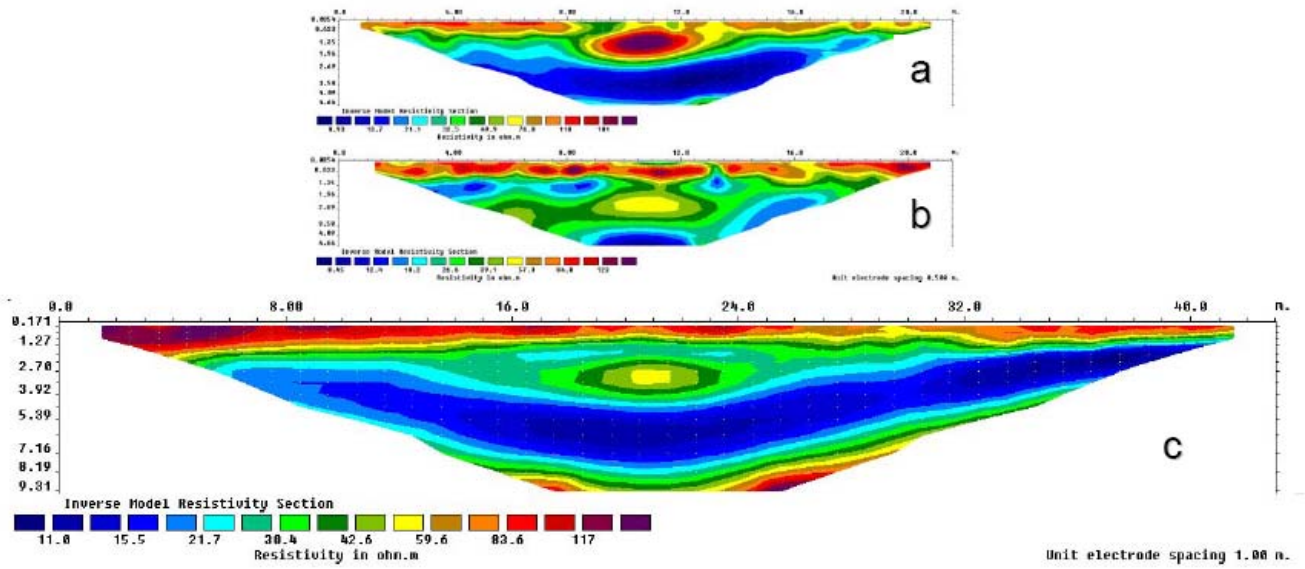

Figure 2: Scaled electrical resistivity profiles acquired across the Ber Juan Spillway tunnel at tunnel depths of (a) 0.90 m, (b) 2.15 m and (c) 3.13 m, respectively. Horizontal and vertical scales are in meters.

Surface Wave Analysis

Data Acquisition

The Rayleigh (surface) wave data were acquired using a Seistronix RAS-24 seismograph and 24-channel streamer consisting of 4.5 Hz geophones spaced at 0.5 m. A 10 kg sledge hammer source with a near-offset of 6 m was employed. Surface wave data were acquired along three parallel traverses oriented perpendicular to the axis of the tunnel. The tunnel was crossed at depths of 0.90, 2.15 and 3.13 m, respectively. ReflexW seismic software was used for pre-processing, editing, visualization and 1D/2D spectrum analysis. The average Rayleigh-wave phase velocity of the upper 3 m of shallow soil was ~160 m/s.

Common Shot Gathers

The location of the tunnel (immediately beneath trace 6) can be estimated from the analyses of the common-shot gathered field data (Figure 3). More specifically, the shallowest surface waves are significantly lower amplitude to the right of trace 6 than to the left as a result of tunnel-related attenuation. Also, backscattered (reflected/diffracted) surface wave energy, characterized by negative apparent velocities (reverse dip), is identified on traces 1-5.

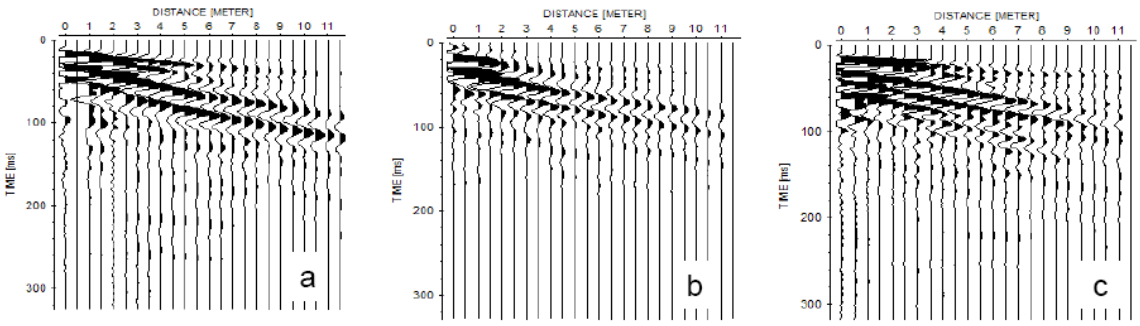

Figure 3: (a) 2D Rayleigh wave profile above the known Ber Juan spillway tunnel at 0.90 m embedment depth; (b) at 2.15 m depth; (c) at 3.13 m depth. The tunnel is located immediately below trace 6. The shallowest surface waves are significantly lower amplitude to the right of trace 6 than to the left as a result of tunnel-related attenuation. Also, backscattered (reflected/diffracted) surface wave energy, characterized by negative apparent velocities (reverse dip), is identified on traces 1-5.

Velocity Filter to Enhance Back-Scattered Energy

Surface wave energy is reflected/diffracted from shallow tunnels. On common gathered data, diffracted/reflected surface waves are characterized by hyperbolic arrival times (Figure 4). To accentuate diffracted/reflected surface-wave energy, an F-K filter was applied to the common shot gathered data (Figure 4). Xia et al. (2006) present a simple method to detect and characterize voids directly from a filtered common shot gather.

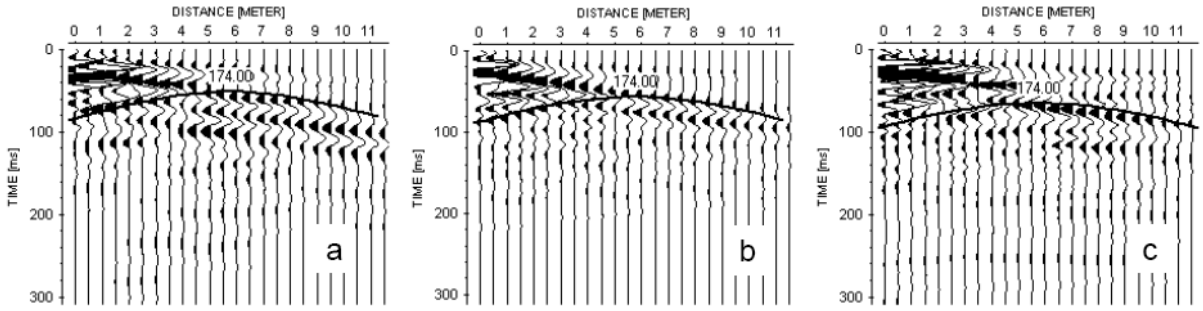

Figure 4: (a) F-K filtered common shot gathered data (a) tunnel at 0.90 m embedment depth; (b) at 2.15 m depth; (c) at 3.13 m depth. The locations of the tunnel are coincident with the apex of the respective arrival-time hyperbola.

To illustrate Xia's approach, consider Figure 4c. The depth to the top of the tunnel can be estimated using the two-way travel time t_o (to apex of the hyperbolic; 0.065 ms), the arrival time of the hyperbolic event at trace 2 (0.080 ms), and the average phase velocity of the shallow soil (160 m/s). Although this approach appears to be very reasonable, the output depth estimates are not always as reliable as one might hope. Using the above input values, the depth to the top of the tunnel imaged on Figure 4c was

estimated to be 1.8 m, whereas it is known to be 3.13 m. Giles et al. (2005) in his numerical modeling results, reports that cavities with circular sections generate less diffraction than rectangular sections.

Spiking Filter Analysis on Common Shot Data

The spiking filter analysis used in this study is described as an algorithm that compares the measure of energy response of the geophones nearest the source to the remaining geophones in the array. In essence, the common shot gather is deconvolved to the first geophones. If there is no anomaly within the region between the excitation pulse and the last geophone, the spiking filters designed on the first few geophones will deconvolve the responses from all the geophones. However, if an anomaly (such as a void) does exist, the resulting reflections and diffractions will disturb the geophone responses such that a spiking filter designed from one response will be unable to properly deconvolve the others. We form a so-called spiking statistic from the ratio of energies after and before application of the spiking filters for each shot. A high spiking statistic indicates there is an anomaly present in the shot preventing effective deconvolution, thus indicating the presence of a void.

Figure 5 below shows the results of the algorithm applied to data collected where the geophone spacing was 0.5 meters. As the geophone array was dragged across the area oriented perpendicular to the tunnel, shots were taken at 0.5 meter intervals. The difference in energy is recorded. Subsequent common shot gathers build a virtual common offset profile. The figure depicts excitation over the tunnel at the 7th shot, the first array geophone was over the tunnel on the 13th shot and the last array geophone was over the tunnel on the 37th shot.

Figure 5: 'Spiking' statistic peaks are noted just after the excitation passes over the tunnel at shot 7. The array spacing was 0.5 m and offset 3 m.

Attenuation Analysis of Rayleigh Waves (AARW)

Numerical studies showed that a rectangular void starts to vibrate in response to the Rayleigh wave excitation and due to the void vibration energy partitioning occurs (Nasseri-Moghaddam et. al. 2006). Part of the incident energy is reflected in the form of Rayleigh wave, another part is converted to body waves and spreads into the medium. Another part of energy is trapped in the void region and bounces back and forth between the void boundaries, until it damps. Therefore, the transferred part of the energy is attenuated and has smaller amplitudes. The trapped energy is associated to higher modes of Rayleigh waves and excited Lamb waves. The effects of reflected and trapped energies are seen as a region in the vicinity of the void with concentrated energy, both in time and frequency domains. The extent of this region depends on the void size, and the frequency content of the incident energy. Thus, in some cases it is possible to correlate the size of the model to the extents of the region with energy concentration.

A technique known as Attenuation Analysis of Rayleigh Waves (AARW) was proposed to determine the location of a void, and estimate its embedment depth (Nasseri-Moghaddam et al. 2005). This technique is based on the observed damping effect of the void on the surface responses. In summary, the method suggests to calculate the cumulative energy of the responses at the location of each receiver over the reliable frequency range (energy-distance parameter - NED) and plotting it versus distance. The location of the peak of the graph corresponds to the void location. To estimate the embedment depth of the void the logarithmic decrement of the frequency data obtained from subsequent receivers are calculated. A summation of the obtained value is carried out over the distance (CALD parameter) and the obtained parameter is plotted verses frequency. The plot fluctuate up to a certain frequency (cutoff frequency) that its wavelength is associated to the embedment depth of the void. Nasseri-Moghaddam (2006) presents the details of the method along its application to the data obtained from numerical models.

Figure 6 shows the contour plot of the collected data over Ber Juan tunnel in time domain. The horizontal axis represents time and vertical axis shows the distance from source. In this case the distance between the source and the first receiver is 1 m. The dashed lines show the projected boundaries of the void on the surface. The measured Rayleigh wave velocity before the void is about 170 m/s. It is seen that larger wave velocities are measured after the void (slope of the events are larger). Previous studies using numerical models and rectangular voids showed similar results over the void. The nature of this behavior is under further study. In the time domain data clear indications of the void such as reflections or amplitude increase in the void region are not seen. Figure 7 shows the same data in frequency domain. These data are multiplied by a gain function to eliminate the effect of geometrical damping. The effect of void is seen in the form of energy concentration before and close to the void. Further, a region with small frequency amplitudes (damped region) is observed after the void. Contrary to the previous experiences (Nasseri-Moghaddam, 2006) the energy concentration before the void – that is associated to the reflected waves – is more visible than the one over the void. The latter differences between this figure and the ones obtained from numerical models can be

associated to the differences between the shape of the tunnel and the shape of the void in the investigated numerical models.

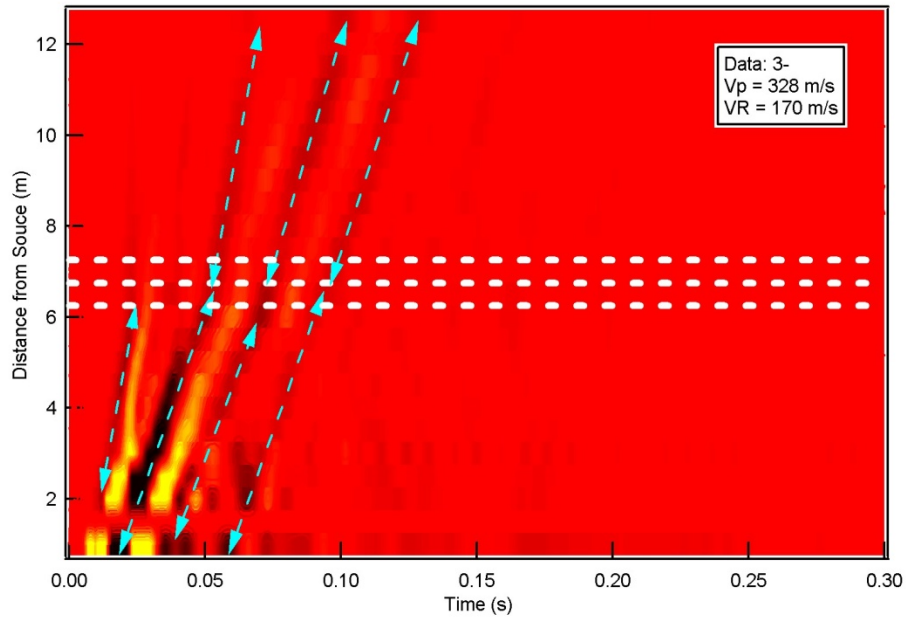

Figure 6: Contour plot of the data collected over Ber Juan spillway tunnel at 0.90 m depth in time domain. The dashed lines show the near boundary, centerline and the far boundary of the tunnel.

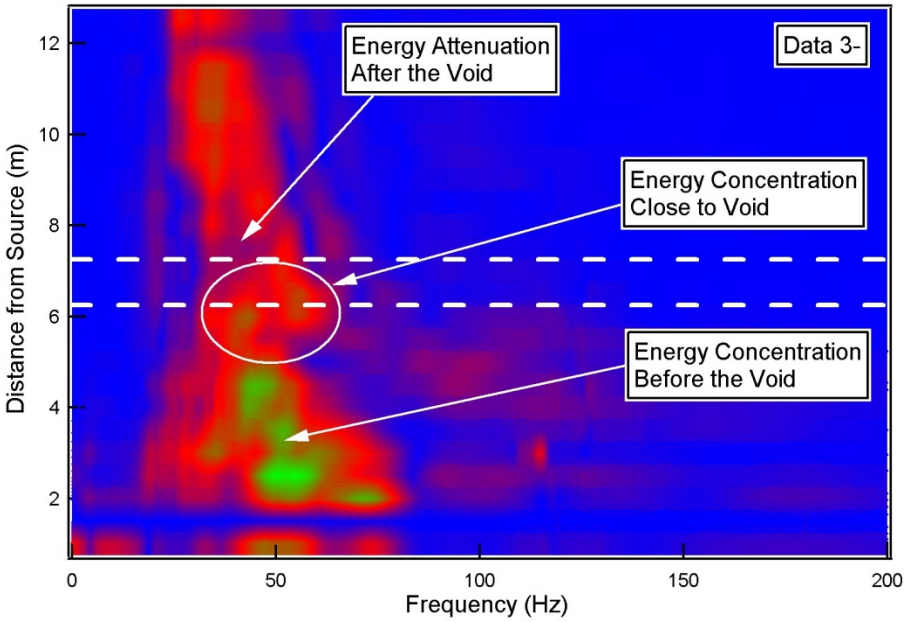

Figure 7: Contour plot of the data collected over Ber Juan spillway tunnel at 0.90 m depth in frequency domain. The dashed lines show the near boundary, centerline and the far boundary of the tunnel.

To locate the void the normalized energy distance parameter (NED) parameter is calculated and plotted versus distance (Figure 8a). The near and far boundaries of the tunnel are shown as vertical dashed lines. A peak with a sharp decrease in the value is seen right at the near boundary of the void, which is an indication of the location of the void. However due to the existence of high energy concentrations before the void (in frequency domain) the maximum peak of this curve occurs before the void location. Figure 8b shows the cumulative amplified logarithmic decrement (CALD) versus frequency. A sharp change in the slope of curve is observed at approximate frequencies 85 Hz and 170 Hz, with wavelengths equal to 2 m and 1 m. These wavelengths are associated to the depth to the top and bottom of the tunnel.

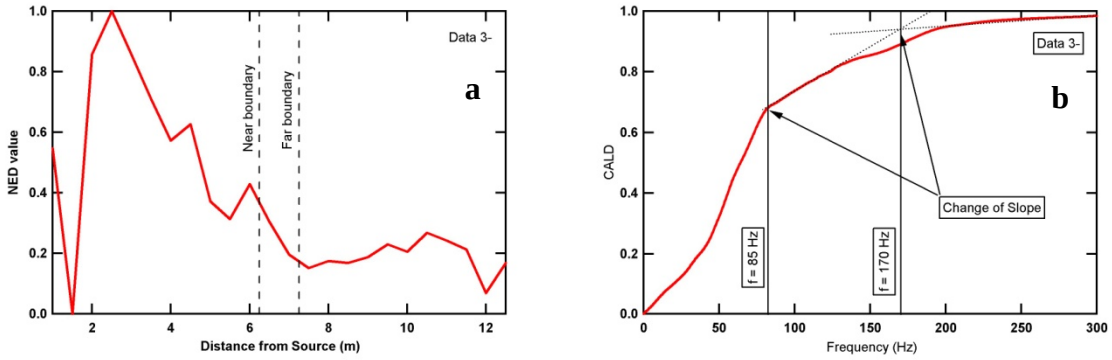

Figure 8: a) The normalized energy distance parameter (NED) verses distance from source. b) The cumulative amplified logarithmic decrement (CALD) value with frequency. Changes in the slope of the curve are observed at f = 85 Hz and 170 Hz, which their wavelengths correspond to the depth to the top and bottom of the tunnel.

Summary and Conclusions

Common shot gathered Rayleigh wave data were acquired. These data were visually analyzed after an F-K filter was applied to enhance diffracted/reflected energy. AARW and Spiking Filter methods were applied to the common shot data to estimate tunnel parameters. Complementary resistivity confirmed the encompassing soil was relatively uniform. The known dimensions of the site were available for comparison through design drawings and on-site tape measurements.

The analytical results were compared using a MATLAB routine to plot the geospatial estimates of tunnel locations (Figure 9b). The redundancy of using this multi-method Rayleigh wave approach reduces the risk of inconclusive or erroneous data interpretation.

Analyses of the common shot gathered data (before and after the application of an F-K filter) illustrates that tunnels at the Ber Juan site can be visually detected on field data at diameter to depth ratios as low as 1 to 3. The AARW and Spiking Filter methods

appear to have significant potential in terms of the automated detection of tunnels. In our opinion, further work to quantifiably characterize tunnels in the Earth's shallow subsurface using a multi-method Rayleigh wave approach is warranted.

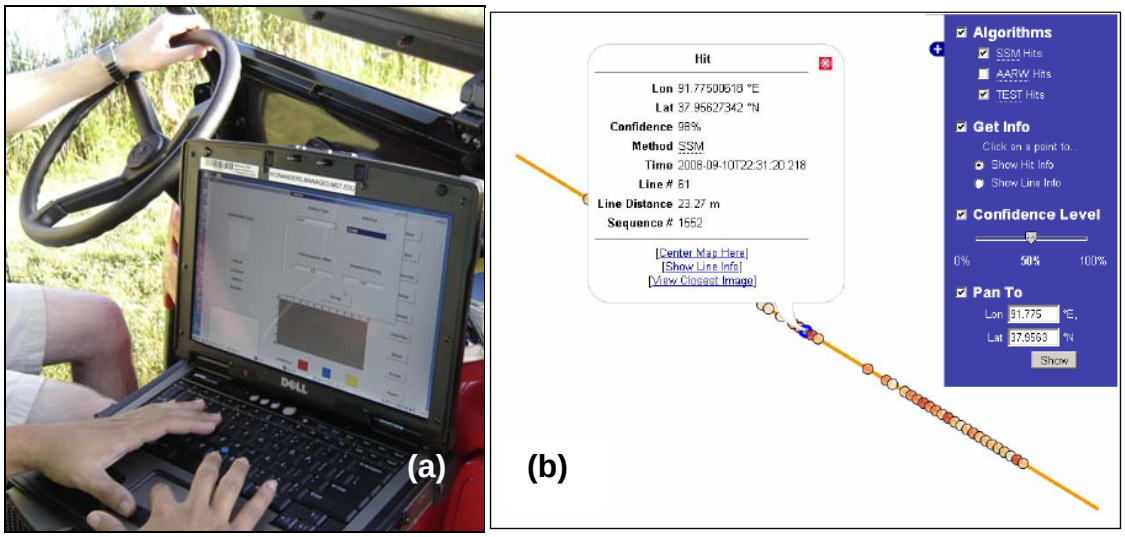

Figure 9: (a) *Laptop with Seismic Interpretation Software: Here the operator is setting the parameters (e.g. length of the line and location of the unit) before beginning the survey;* (b) *Mapping Tool (Screen Capture) that plots anomaly based on AARW and Spiking Analysis where certainty is based on relative algorithm strength value of the anomaly.*

The funding for this research and development was provided through the Leonard Wood Institute from the U. S. Army Research Laboratory.

References

Giles, C., Leparoux, D., Virieux, J., Bitri, A., Operto, S., and Grandjean, G., 2005, Numerical modeling of surface waves over shallow cavities: Journal of Environmental and Engineering Geophysics, 10(2), 111-121.

Miller, R., Park C., Xia, J., Ivanov, J., and Steeples, D., 2006, Tunnel Detection Using Seismic Methods: 2006 Joint Assembly of the American Geophysical Union, Baltimore: NS21A-07.

Nasseri-Moghaddam, A., 2006, Study of the Effect of Lateral Inhomogeneities on the Propagation of Rayleigh Waves in an Elastic Medium, Canada, University of Waterloo: Ph.D. Thesis.

Reynolds, John M., 2000, An Introduction to Applied and Environmental Geophysics, England, Wiley & Sons, Ltd..

Xia, J., Nyquist, J. E., Xu, Y., and Roth, M. J. S., 2006. Feasibility of Detecting Voids with Rayleigh Wave Diffraction, Pennsylvania: 2006 Philadelphia Annual Meeting of the Geological Society of America, Paper 218-7. http://gsa.confex.com/gsa/2006AM/finalprogram/session_18007.htm See 218-7.